



Revisiting properties and concentrations of ice nucleating particles in the sea surface microlayer and bulk seawater in the Canadian Arctic during summer

Victoria E. Irish¹, Sarah Hanna¹, Yu Xi¹, Matthew Boyer², Elena Polishchuk¹, Jessie Chen¹, Jonathan P.D. Abbatt³, Michel Gosselin⁴, Rachel Chang², Lisa Miller⁵, Allan K. Bertram¹

¹ Department of Chemistry, University of British Columbia, 2036 Main Mall, Vancouver, BC V6T 1Z1, Canada

² Department of Physics and Atmospheric Science, Dalhousie University, Sir James Dunn Building, 6310 Coburg Road, Halifax, Nova Scotia, B3H 4R2, Canada

³ Department of Chemistry, University of Toronto, 80 St George Street, Toronto, Ontario, ON M5S 3H6, Canada

⁴ Institut des sciences de la mer de Rimouski, Université du Québec à Rimouski, 310 Allée des Ursulines, Rimouski, Québec, QC G5L 3A1, Canada

⁵ Institute of Ocean Sciences, Fisheries and Oceans Canada, Sidney, BC V8L 4B2, Canada

Correspondence to: Allan Bertram (bertram@chem.ubc.ca)

Abstract. Despite growing evidence that the ocean is an important source of ice nucleating particles (INPs) in the atmosphere, our understanding of the properties and concentrations of INPs in ocean surface waters remain limited. We have investigated the properties and concentrations of INPs in sea surface microlayer and bulk seawater samples collected in the Canadian Arctic during the summer of 2016. We observed that 1) INPs were ubiquitous in the microlayer and bulk waters; 2) heat and filtration treatments reduced INP activity, indicating that the INPs were likely heat-labile biological materials between 0.2 and 0.02 μm in diameter; 3) there was a strong negative correlation between salinity and freezing temperatures, possibly due to INPs associated with melting sea ice; and 4) concentrations of INPs could not be explained by satellite-derived chlorophyll *a* concentrations. Although the spatial patterns of INPs and salinities were similar in 2014 and 2016, we did observe some differences between the years, notably: 1) the concentrations of INPs were higher on average in 2016 compared to 2014; and 2) INP concentrations were enhanced in the microlayer compared to bulk seawater in several samples collected in 2016, which was not the case in 2014.

1 Introduction

Ice-nucleating particles (INPs) are atmospheric particles that catalyse the formation of ice crystals in clouds at warmer temperatures and lower saturations than needed for homogeneous ice nucleation, thereby influencing cloud properties and potentially impacting the Earth's radiative properties and hydrological cycle (Boucher et al., 2013; Lohmann, 2002; Lohmann and Feichter, 2005; Tan et al., 2016). Only a small subset of atmospheric particles (about 1 in 10^6) act as INPs (DeMott et al., 2010, 2016). INPs can catalyse the formation of ice by four different mechanisms: contact freezing,



condensation freezing, deposition freezing, and immersion freezing. Immersion freezing, which is the focus of this paper, occurs when an INP immersed in a supercooled water droplet initiates the freezing process.

One potential source of INPs to the atmosphere is the ocean. Oceans dominate the Earth's surface cover, and sea spray generates a large fraction of the aerosol mass in the atmosphere (Lewis and Schwartz, 2004). Several pieces of evidence suggest that the ocean is an important source of INPs to the atmosphere. For example, INPs have been measured in seawater or the sea surface microlayer (herein referred to as microlayer) (Fall and Schnell, 1985; Irish et al., 2017; Rosinski et al., 1988; Schnell, 1977; Schnell and Vali, 1975, 1976; Wilson et al., 2015) and in the air above the ocean (Bigg, 1973; Rosinski et al., 1986, 1987, 1988). Marine microorganisms and their by-products can also catalyse ice formation (Burrows et al., 2013; Knopf et al., 2011; Rosinski et al., 1987; Wilson et al., 2015). In addition, modelling studies have illustrated that INP concentrations from the ocean can be important when other sources of INPs, such as mineral dust, are low (Yun and Penner, 2013).

Despite growing evidence that the ocean is an important source of INPs in the atmosphere, our understanding of the properties and concentrations of INPs in the microlayer and bulk seawater remain limited. For example, information on the spatial and temporal distributions of INPs in the microlayer and bulk seawater has not been investigated in any detail. Nevertheless, this type of information is needed to improve predictions of INP emissions to the atmosphere from the ocean. Recently, we reported the properties and concentrations of INPs in the microlayer and bulk seawater collected in the Canadian Arctic during the summer of 2014 (Irish et al., 2017). We found INPs were ubiquitous in the microlayer and bulk seawater. Heat and filtration treatment of the samples indicated that the INPs were likely heat-labile biological materials with sizes between 0.02 and 0.2 μm in diameter. In addition, we found that the freezing activity of the microlayer and bulk seawater samples was inversely correlated with salinity, possibly because the INPs were associated with melting sea ice. We also observed that the freezing properties in the microlayer were similar to those of the bulk seawater, in almost all samples. Building on our previous studies, we returned to the Canadian Arctic during the summer of 2016 to further investigate the properties and concentrations of INPs in Arctic Ocean waters. Locations where samples were collected during both years are indicated in Fig. 1, and the detailed sampling dates and locations in 2016 are given in Table 1. By comparing results from 2016 with results from 2014, we investigate whether the properties, concentrations and spatial profiles of the INPs vary from year-to-year at similar locations. This type of information is needed to understand and predict concentrations of INPs in the atmosphere.

2 Experimental

2.1 Collection methods

During July and August of 2016 samples were collected from the eastern Canadian Arctic on board the CCGS *Amundsen* as part of the NETCARE project (Fig. 1 and Table 1). Supplementary details, including notes and photographs taken at each sampling station, are provided in Table S1.



2.1.1 Automated sampler method

In contrast to 2014, when we collected microlayer samples manually using a glass plate sampler (Irish et al., 2017), in 2016, microlayer samples were collected using rotating glass plates attached to an automated sampling catamaran (Shinki et al., 2012). At station 1, the automated sampling catamaran was deployed from a small inflatable, rigid-hull boat at least 500 m away from the CCGS *Amundsen*. The automated sampling catamaran was remotely driven at least 20 m away from the small inflatable, rigid-hull boat before the rotating glass plates were activated. A rotation rate of 10 revolutions per minute was used. From station 2 onwards, the automated rotating glass plates on the sampling catamaran experienced technical problems. Subsequently, the automated sampling catamaran was kept on the upwind side of the small inflatable, rigid-hull boat with its engine turned off, at least 500 m away from the CCGS *Amundsen* to avoid contamination, and the glass plates were rotated manually between 11 to 18 revolutions per minute. Even though manual rotation was used, for convenience, we will refer to the method as “automated sampling”, and the instrument as an “automated sampler” in all cases. The microlayer that adhered to the plates from each rotation was scrapped off with fixed Teflon wiper blades into a manifold and then pumped through Teflon tubing into high-density polyethylene (HDPE) Nalgene bottles (ranging from 250 mL to 2 L in size). The thickness of the microlayer collected was approximately 80 μm based on the rotation rate (between 11 - 18 revolutions per minute), the average volume collected (3000 mL) and an average collection time (18 minutes). Bulk seawater samples were collected at the same times and locations as the microlayer samples through Teflon tubing suspended 0.2 m below the automated sampler. The bulk seawater was pumped, using peristaltic pumps, into HDPE Nalgene bottles (ranging from 250 mL to 2 L in size). After collection, the Nalgene bottles containing the microlayer and bulk seawater samples were kept cool in an insulated container. Upon returning to the ship, the samples were homogenised by gently (so as to not break up cells that may be present in the samples) inverting them at least ten times and then sub-sampled into smaller bottles for subsequent analyses.

The glass plates, aluminium manifold, Teflon tubing and all Nalgene bottles were sterilised first with bleach, then cleaned with isopropanol and finally rinsed with ultrapure water. After cleaning, the sampler was further rinsed by collecting then discarding microlayer and bulk seawater for approximately 2 minutes, before samples were retained. Procedural blanks were prepared by running approximately 1 L of ultrapure water through the sample tubing on the automated sampler for approximately 1 minute.



2.2 Ice nucleation properties of the samples

2.2.1 Droplet freezing technique and INP concentrations

INP concentrations as a function of temperature were determined using the droplet freezing technique (DFT; Koop et al., 1998; Vali, 1971; Whale et al., 2015; Wilson et al., 2015). Sub-samples of the microlayer and bulk seawater were kept in 15 mL polypropylene tubes between 1 to 4 °C for a maximum of 4 hours before INP analysis.

In the freezing experiments three hydrophobic glass slides (Hampton Research, Aliso Viejo, CA, USA) were placed directly on a cold stage (Whale et al., 2015) and between 15 to 30 droplets of the sample, with volumes of 1 µL each, were deposited onto each of the glass slides using a pipette. A chamber with a webcam attached to the top of it was placed over the slides to isolate them from ambient air, and a flow of ultrapure N₂ was passed through the chamber as described by Whale et al. (2015). The droplets were cooled at a constant rate of 10 °C/min from 0 °C to -35 °C and the webcam recorded videos of the droplets during cooling. All videos were analysed by the DFT to determine the freezing temperature of each droplet. For comparison, ultrapure water (distilled water further purified with a Millipore system, 18.2 MΩcm at 25 °C), as well as the procedural blanks, were analysed for INPs using the DFT.

The concentration of INPs, [INP(T)] (L⁻¹), was determined from each freezing experiment by the following equation (Vali, 1971):

$$[\text{INP}(T)] = -\ln\left(\frac{N_u(T)}{N_o}\right) N_o \cdot \frac{1}{V} \quad (1)$$

Where $N_u(T)$ is the number of unfrozen droplets at temperature T , N_o is the total number of droplets used in the experiment, and V is the volume of all droplets in a single experiment. This equation accounts for the possibility of multiple INPs contained in a single droplet.

2.2.2 Heating and filtration tests

The freezing temperatures of the microlayer and bulk seawater samples were also measured after they had been passed through syringe filters with three different pore sizes (Whatman 10 µm pore size PTFE membranes, Millex-HV 0.2 µm pore size PTFE membranes, and Anotop 25 0.02 µm pore size inorganic Anopore™ membranes) (Irish et al., 2017; Wilson et al., 2015). The sub-samples of the microlayer and bulk seawater were left for a maximum of 4 hours before filtration and INP analysis.

The freezing temperatures of the microlayer and bulk seawater samples were also measured after they had been heated to 100 °C (Christner et al., 2008; Irish et al., 2017; Schnell and Vali, 1975; Wilson et al., 2015). In this case, samples were stored at -80 °C for less than 6 months and analysed in the laboratory at the University of British Columbia. Before heating



the stored samples, they were completely thawed and homogenised by inverting at least ten times. Then the freezing temperatures were determined after heating the samples at 100 °C for approximately an hour.

Separate experiments show that storage of the samples at -80 °C for a maximum of six months does not affect the INP concentration in microlayer and bulk seawater samples (see Fig. S1 in the Supplement).

5

2.2.3 Corrections for freezing temperature depression

The measured freezing temperatures were adjusted for the depression of the freezing point by the presence of salts to generate freezing temperatures applicable to salt-free conditions (salinity = 0 g kg⁻¹), which is relevant for mixed phase clouds. In short, water activities of the samples were calculated from measured salinities using an Aerosol Thermodynamic Model (<http://www.aim.env.uea.ac.uk/aim/aim.php>; Friese and Ebel, 2010; Wexler and Clegg, 2002). Next, the water activity of an ice-salt solution at the median freezing temperature was calculated. The freezing temperature at salinity = 0 g kg⁻¹ was then calculated from the difference in these two water activities following the procedure of Koop and Zobrist (2009).

The salinities of the microlayer and bulk seawater samples were measured within 10 minutes of sample collection using a hand-held salinity probe (SympHony; VWR, Radnor, PA, USA). The salinities (measured in practical salinity units (psu)) were corrected after collection using a linear fit to salinometer readings. The correction for freezing point depression by the presence of salts based on the measured salinities ranged from 1.2 to 2.6 °C.

2.3 Bacterial and phytoplankton abundance

The abundances of heterotrophic bacteria and phytoplankton < 20 µm (i.e., phycoerythrin-containing cyanobacteria, phycocyanin-containing cyanobacteria and autotrophic eukaryotes) were measured by flow cytometry. Duplicate 4 mL subsamples were fixed with glutaraldehyde (Grade I; 0.12 % final concentration; Sigma-Aldrich G5882) in the dark at room temperature for 15 min, flash-frozen in liquid nitrogen and then stored at -80 °C until analysis. Samples for heterotrophic bacteria enumeration were stained with SYBR Green I (Invitrogen) following Belzile et al. (2008). Bacteria were counted with a BD Accuri C6 flow cytometer using the blue laser (488 nm). The green fluorescence of nucleic acid-bound SYBR Green I was measured at 525 nm. Archaea could not be discriminated from Bacteria using this protocol; therefore, hereafter, we use the term bacteria to include both Archaea and Bacteria with high nucleic acid (HNA) content and low nucleic acid (LNA) content. Samples for < 20 µm phytoplankton abundances were analyzed using a CytoFLEX flow cytometer (Beckman Coulter) fitted with a blue (488 nm) and red laser (638 nm), using CytoExpert v2 software. Using the blue laser, forward scatter, side scatter, orange fluorescence from phycoerythrin (582/42 nm BP) and red fluorescence from chlorophyll (690/50 nm BP) were measured. The red laser was used to measure the red fluorescence of phycocyanin (660/20 nm BP).



Polystyrene microspheres of 2 μm diameter (Fluoresbrite YG, Polysciences) were added to each sample as an internal standard (Marie et al., 2005; Tremblay et al., 2009).

2.4 Chlorophyll *a* satellite data

5 Chlorophyll *a* concentrations for case 1 waters (waters dominated by phytoplankton) were retrieved from the GlobColour project website (<http://globcolour.info>, *ACRI-ST, France*). The GlobColour project provides a high resolution, long time-series of global ocean colour information by merging data from several satellite systems. For the data used here, these include either or both of: the Moderate Imaging Spectrometer (MODIS) on the Aqua Earth Observing System (EOS) mission; and the Visible/Infrared Imager Radiometer Suite (VIIRS) aboard the Suomi National Polar-orbiting Partnership
10 satellite. The GlobColour project merges data from multiple satellite systems in several different ways. For this work we used data merged with weighted averaging, where weightings are based on the sensor and/or product. Data are available at daily, 8-day, and monthly resolutions. In this study 8-day data were used to achieve the best balance between complete spatial coverage and high time resolution. Spatial resolution is $1/24^\circ$ (~ 4 km). To determine the chlorophyll *a* concentration at a given sampling location, we used the grid cell containing that station.

15

2.5 Statistical analysis

Pearson correlation analysis was applied to many of the variables measured in this study to compute correlation coefficients (*r*). *P* values were also calculated to determine the significance of the correlations at the 95 % confidence level ($p < 0.05$).

20 3 Results and Discussion

3.1 Concentrations of INPs

The frozen fraction curves for all microlayer and bulk seawater samples are shown in Fig. S2 in the Supplement. Also shown for comparison are the fraction frozen curves for ultrapure water and ultrapure water passed through the tubing in the automated sampler (the procedural blanks). In addition, the frozen fraction curves of the samples after passing through a 0.02
25 μm Anotop 25 syringe filter are shown.

For the bulk seawater, all untreated samples froze at temperatures warmer than ultrapure water. Freezing temperatures as warm as -6 °C were observed. In addition, the bulk seawater samples also froze at warmer temperatures than the procedural blanks. These results indicate the presence of ice-active material in all bulk seawater samples.



For the microlayer samples, all samples froze at temperatures warmer than ultrapure water. These results also suggest that all microlayer samples contained ice-active material. For some microlayer samples, some of the freezing temperatures were lower than the freezing temperatures of the procedural blanks. However, the freezing temperatures of the procedural blanks should be viewed as an upper limit to the background freezing temperatures, since prior to collecting the blanks, the sampler had not been rinsed as thoroughly as before collecting the microlayer samples.

The median temperatures at which 50 % of the droplets froze in the microlayer and bulk seawater samples were $-18.6\text{ }^{\circ}\text{C}$ and $-21.1\text{ }^{\circ}\text{C}$, respectively, in 2016. In contrast, in 2014, the median temperatures at which 50 % of the droplets froze in the microlayer and bulk seawater samples were lower at $-27.1\text{ }^{\circ}\text{C}$ and $-27.3\text{ }^{\circ}\text{C}$, respectively.

In Fig. 2, the concentrations of INPs, [INP(T)], measured in 2016 are compared with concentrations measured in 2014, also in the Canadian Arctic. In both 2016 and 2014 the concentrations of INPs vary by at least 2 orders of magnitude at one temperature, but on average concentrations measured in 2016 were higher than the concentrations measured in 2014.

Shown in Fig. 3 is the correlation between T_{10} -values (temperatures at which 10 % of the droplets froze) in the microlayer and bulk seawater samples from 2016. A strong positive correlation ($r = 0.89$ and $p < 0.001$) was observed between the freezing properties of the microlayer and the freezing properties of the bulk seawater, consistent with our previous observations (Irish et al., 2017). In 2016, 5 out of 11 samples had warmer T_{10} -values in the microlayer compared to bulk seawater. However, in the 2014 samples, only 1 out of 8 samples had warmer T_{10} -values in the microlayer compared to bulk seawater (Irish et al., 2017). The difference between 2016 and 2014 may simply be due to year-to-year variations in the properties of the microlayer relative to the bulk seawater related to variations in oceanic conditions. For example, Collins et al. (2017) documented differences in the activity of marine microbial communities between 2016 and 2014 in the Canadian Arctic. In addition, the differences between 2016 and 2014 may be related to sampling techniques. In 2014 the glass plate technique collected a layer that was up to $220\text{ }\mu\text{m}$ thick. In contrast, in 2016 a thinner layer (approximately $80\text{ }\mu\text{m}$ thick) was collected. In the thicker layers collected in 2014, the microlayer INPs would have been diluted by bulk waters. Additional studies of how INP activity varies as a function of microlayer sample thickness are necessary to resolve this issue.

3.2 Effect of heating and filtering the samples

Figure S3 shows that the frozen fraction curves were shifted to colder temperatures after the microlayer and bulk seawater samples were heated to $100\text{ }^{\circ}\text{C}$. These results are similar to what we observed for the 2014 samples (Irish et al., 2017). This suggests that the ice-active material we found in the microlayer and bulk seawater samples was likely heat-labile biological material (Christner et al., 2008).

Figure S4 shows that the temperature at which droplets had frozen in microlayer and bulk seawater samples significantly decreased after the samples were filtered with a $0.02\text{ }\mu\text{m}$ filter, but not with 10 or $0.2\text{ }\mu\text{m}$ filters. A similar result was observed in the 2014 samples (Irish et al., 2017), suggesting that the INPs in the microlayer and bulk seawater were between $0.2\text{ }\mu\text{m}$ and $0.02\text{ }\mu\text{m}$ in size.



3.3 Spatial patterns of INPs in the Canadian Arctic

The spatial patterns of T_{10} -values and salinities for bulk seawater samples in both 2016 and 2014 are shown in Fig. 4. The same spatial patterns, but for microlayer samples, are shown in Fig. S5. Spatial pattern of salinities, in addition to the T_{10} -values, are shown since salinities were the strongest predictor of freezing in the samples (see Sect. 3.4). In each panel the colour scales have been adjusted to easily compare the general pattern of T_{10} -values and salinities between years. For both 2014 and 2016, the T_{10} -values for samples taken from northern Baffin Bay and Nares Strait between Greenland and Canada, above 75 °N, are generally lower than the T_{10} -values elsewhere. On the other hand, for the same samples, the salinities are generally higher than salinities we observed elsewhere.

To further investigate the similarities in spatial patterns between 2014 and 2016, a comparison was made of T_{10} -values and salinities for sampling sites in close proximity for the two years. Labeled in Fig. 5a are sampling sites in 2014 and 2016 identified as being in close proximity. A strong positive correlation ($r = 0.9$, $p < 0.001$) was found between the T_{10} -values measured in 2014 and T_{10} -values measured in 2016 when comparing locations in close proximity (Fig. 5b), suggesting that the spatial patterns of T_{10} -values measured in 2014 and 2016 were similar even though on average T_{10} -values were higher in 2016. In addition, a strong positive correlation ($r = 0.78$, $p \leq 0.001$) was found between the salinities measured in 2014, and salinities measured in 2016 when comparing locations in close proximity (Fig. 5c), which suggests that we sampled similar water masses in both years at those locations.

3.4 Correlations with biological and physical properties of microlayer and bulk seawater

In Table 2 and Fig. 6, we present correlations between T_{10} -values from bulk seawater and heterotrophic bacterial abundance, phytoplankton (including 0.2-20 μm photosynthetic eukaryotes and cyanobacteria) abundance, salinity and temperature for the 2016 data. The strongest relationships with T_{10} -values for both the bulk and microlayer samples were with salinity (bulk: $r = -0.83$, $p \leq 0.001$; microlayer: $r = -0.74$, $p < 0.01$). As discussed by Irish et al. (2017), a possible explanation for the negative correlation between salinity and freezing temperature is that the INPs are associated with sea-ice melt. Melting sea ice not only decreases surface ocean salinity, but can also release sea-ice microorganisms, such as sea-ice diatoms and bacteria, and their exudates that may serve as effective INPs (Assmy et al., 2013; Boetius et al., 2015; Ewert and Deming, 2013; Fernández-Méndez et al., 2014). Also interesting, a strong negative correlation was observed between T_{10} -values in bulk seawater and bacterial abundance ($r = -0.77$, $p < 0.01$). A higher concentration of bacteria has been observed in the open sea compared to melt ponds, and bacteria produce copious amounts of exopolymers when they are stressed during melting processes (Galgani et al., 2016). Although there may be fewer bacteria in melting sea-ice, these bacteria may be stressed by the melting process and produce exopolymers that could act as INPs.



Terrestrial run-off (including that from melting glaciers and permafrost) also decreases salinity, and could be a source of ice nucleating material to the surface ocean (Christner et al., 2008). An analysis of water masses in our study area during 2014 showed that in some areas of our study, there could be substantial influence of non-sea-ice fresh water, particularly in Hall Basin and Kane Basin within Nares Strait (Burgers et al., 2017). However, the low T_{10} -values we observed at the northernmost stations that were surrounded by the most glaciers around Kane Basin and Nares Strait (refer back to Sect. 3.3 and Fig. 4 for further details) indicate that terrestrial freshwater is not the most important source of efficient INPs in the microlayer of this area.

Another possible explanation for the negative correlation between salinity and INPs is a non-colligative effect of sea salt on the freezing temperature. Solutes can impact freezing temperature by blocking INP active sites (Kumar et al., 2018). To test this hypothesis, we varied the salinity in one of the microlayer samples (station 4) by adding commercial sea salt (Instant Ocean™), while keeping the concentration of ice nucleating material in the samples constant (see Supplement Sect. 1 for more details). The T_{10} -values for these salinity-enhanced samples (after correcting for freezing point depression) varied by less than the uncertainty in the measurements as the salinity of the sample was increased from 29 to 55 g/kg (Fig. S6 in the Supplement). These results suggest that sea salt does not have a non-colligative effect on the freezing temperature of the samples, at least not for the microlayer sample tested (station 4). Consistent with these results, non-colligative effects have not been observed in previous studies of immersion freezing with seawater and salt solutions (Alpert et al., 2011a, 2011b; Knopf et al., 2011; Wilson et al., 2015; Zobrist et al., 2008).

3.4.1 Chlorophyll *a* satellite data correlations

Figure 7 shows correlations between the chlorophyll data retrieved from GlobColour and the T_{10} -values for the microlayer and bulk seawater. The results indicate that correlations between T_{10} -values in the microlayer or bulk seawater and chlorophyll *a* are not statistically significant, consistent with our results from 2014 (Irish et al., 2017). These observations are also consistent with recent work by Wang et al. (2015), who showed that INP concentrations in sea spray aerosol emitted during a mesocosm tank experiment were not simply coupled to chlorophyll *a* concentrations.

25

4 Conclusion

The INP concentrations of microlayer and bulk seawater were determined at eleven stations in the Canadian Arctic during the summer of 2016, and compared to measurements made in 2014 (Irish et al., 2017). Filtration reduced the freezing temperatures of all samples, suggesting ice-active particulate material was universally present in the microlayer and bulk seawaters we studied. Some samples had freezing temperatures as high as -5 °C. Freezing temperatures also decreased after heat treatment indicating that the ice-active material was likely heat-labile biological material, consistent with previous

30



measurements of INPs in the microlayer (Wilson et al., 2015) and bulk seawater (Schnell, 1977; Schnell and Vali, 1975, 1976). The ice-active material we observed in seawater was between 0.2 μm and 0.02 μm in size, also consistent with previous studies of INPs in the microlayer (Wilson et al., 2015) and bulk seawater (Rosinski et al., 1986; Schnell and Vali, 1975).

- 5 We found a strong negative correlation between salinity and freezing temperatures, leading us to hypothesise that INPs are associated with the exudates from sea-ice microorganisms, which are released into the ocean upon sea-ice melt. Chlorophyll *a* concentrations from satellite measurements did not correlate with INP concentrations in seawater, consistent with recent work by Wang et al. (2015) in a mesocosm tank experiment. A possible explanation for these observations is that INP concentrations are not sensitive to the instantaneous photosynthetic productivity of a biological community, but rather to the
- 10 nature of that community, and its life stage, including potential stresses experienced by sympagic communities during sea-ice melt.

When comparing the INP concentrations in the same areas between 2014 and 2016, we found little inter-annual variability in the spatial pattern of INPs or salinity. In 2016, we observed higher concentrations of INPs nucleating ice at higher temperatures, particularly in the microlayer samples, than we did in 2014. This could, in part, be a result of the automated

15 sampler collecting a thinner microlayer in 2016, a hypothesis that could be tested by collecting microlayer samples using both collection methods in the same region at the same time.

Acknowledgements

We would like to thank the scientists, officers, and crew of the CCGS *Amundsen* for their support during the expedition;

20 Lucius Perreault for land-based support with the microlayer sampler; Allison Lapin, Eugene Shen, and Hang Nguyen for help with INP analysis; Joannie Charette, Aude Boivin-Rioux, and Claude Belzile for flow cytometry analysis. We would also like to thank the Natural Sciences and Engineering Research Council of Canada (the NETCARE project), Fisheries and Oceans Canada and ArcticNet (Network of Centres of Excellence of Canada) for funding this work. GlobColour data (<http://globcolour.info>) used in this study were developed, validated, and distributed by ACRI-ST, France.

25



References

- Alpert, P. A., Aller, J. Y. and Knopf, D. A.: Ice nucleation from aqueous NaCl droplets with and without marine diatoms, *Atmos. Chem. Phys.*, 11, 5539–5555, doi:10.5194/acp-11-5539-2011, 2011a.
- Alpert, P. A., Aller, J. Y. and Knopf, D. A.: Initiation of the ice phase by marine biogenic surfaces in supersaturated gas and
5 supercooled aqueous phases, *Phys. Chem. Chem. Phys.*, 13, 19882–19894, doi:10.1039/c1cp21844a, 2011b.
- Assmy, P., Ehn, J. K., Fernández-Méndez, M., Hop, H., Katlein, C., Sundfjord, A., Bluhm, K., Daase, M., Engel, A., Fransson, A., Granskog, M. A., Hudson, S. R., Kristiansen, S., Nicolaus, M., Peeken, I., Renner, A. H. H., Spreen, G., Tatarek, A. and Wiktor, J.: Floating Ice-Algal Aggregates below Melting Arctic Sea Ice, *PLoS One*, 8, e76599, doi:10.1371/journal.pone.0076599, 2013.
- 10 Belzile, C., Brugel, S., Nozais, C., Gratton, Y. and Demers, S.: Variations of the abundance and nucleic acid content of heterotrophic bacteria in Beaufort Shelf waters during winter and spring, *J. Mar. Syst.*, 74, 946–956, doi:10.1016/j.jmarsys.2007.12.010, 2008.
- Bigg, E. K.: Ice Nucleus Concentrations in Remote Areas, *J. Atmos. Sci.*, 30, 1153–1157, doi:10.1175/1520-0469(1973)030<1153:INCIRA>2.0.CO;2, 1973.
- 15 Boetius, A., Anesio, A. M., Deming, J. W., Mikucki, J. and Rapp, J. Z.: Microbial ecology of the cryosphere : sea ice and glacial habitats, *Nat. Rev. Microbiol.*, 13, 677–690, doi:10.1038/nrmicro3522, 2015.
- Boucher, O., Randall, D., Artaxo, P., Bretherton, C., Feingold, G., Forster, P., Kerminen, V.-M., Kondo, Y., Liao, H., Lohmann, U., Rasch, P., Satheesh, S. K., Sherwood, S., Stevens, B. and Zhang, X. Y.: Clouds and aerosols, *Clim. Chang.* 2013 Phys. Sci. Basis Work. Gr. I Contrib. to Fifth Assess. Rep. Intergov. Panel Clim. Chang., 9781107057, 571–658,
20 doi:10.1017/CBO9781107415324.016, 2013.
- Burgers, T. M., Miller, L. A., Thomas, H., Else, B. G. T., Gosselin, M. and Papakyriakou, T.: Surface Water $p\text{CO}_2$ Variations and Sea-Air CO_2 Fluxes During Summer in the Eastern Canadian Arctic, *J. Geophys. Res. Ocean.*, 122, 9663–9678, doi:10.1002/2017JC013250, 2017.
- Burrows, S. M., Hoose, C., Pöschl, U. and Lawrence, M. G.: Ice nuclei in marine air: Biogenic particles or dust?, *Atmos.*
25 *Chem. Phys.*, 13, 245–267, doi:10.5194/acp-13-245-2013, 2013.
- Christner, B. C., Cai, R., Morris, C. E., McCarter, K. S., Foreman, C. M., Skidmore, M. L., Montross, S. N. and Sands, D. C.: Geographic, seasonal, and precipitation chemistry influence on the abundance and activity of biological ice nucleators in rain and snow, *Proc. Natl. Acad. Sci. U. S. A.*, 105, 18854–18859, doi:10.1073/pnas.0809816105, 2008.
- Collins, D. B., Burkart, J., Chang, R. Y. W., Lizotte, M., Boivin-Rioux, A., Blais, M., Mungall, E. L., Boyer, M., Irish, V. E.,
30 Massé, G., Kunkel, D., Tremblay, J. É., Papakyriakou, T., Bertram, A. K., Bozem, H., Gosselin, M., Levasseur, M. and Abbatt, J. P. D.: Frequent ultrafine particle formation and growth in Canadian Arctic marine and coastal environments, *Atmos. Chem. Phys.*, 17, 13119–13138, doi:10.5194/acp-17-13119-2017, 2017.
- DeMott, P. J., Prenni, A. J., Liu, X., Kreidenweis, S. M., Petters, M. D., Twohy, C. H., Richardson, M. S., Eidhammer, T.



- and Rogers, D. C.: Predicting global atmospheric ice nuclei distributions and their impacts on climate., *Proc. Natl. Acad. Sci. U. S. A.*, 107, 11217–11222, doi:10.1073/pnas.0910818107, 2010.
- DeMott, P. J., Hill, T. C. J., McCluskey, C. S., Prather, K. A., Collins, D. B., Sullivan, R. C., Ruppel, M. J., Mason, R. H., Irish, V. E., Lee, T., Hwang, C. Y., Rhee, T. S., Snider, J. R., McMeeking, G. R., Dhaniyala, S., Lewis, E. R., Wentzell, J. J. B., Abbatt, J., Lee, C., Sultana, C. M., Ault, A. P., Axson, J. L., Diaz Martinez, M., Venero, I., Santos-Figueroa, G., Stokes, M. D., Deane, G. B., Mayol-Bracero, O. L., Grassian, V. H., Bertram, T. H., Bertram, A. K., Moffett, B. F. and Franc, G. D.: Sea spray aerosol as a unique source of ice nucleating particles, *Proc. Natl. Acad. Sci.*, 113, 5797–5803, doi:10.1073/pnas.1514034112, 2016.
- Ewert, M. and Deming, J. W.: Sea Ice Microorganisms: Environmental Constraints and Extracellular Responses, *Biology* (Basel), 2, 603–628, doi:10.3390/biology2020603, 2013.
- Fall, R. and Schnell, R. C.: Association of an ice-nucleating pseudomonad with cultures of the marine dinoflagellate, *heterocapsa niei*, *J. Mar. Res.*, 43, 257–265, 1985.
- Fernández-Méndez, M., Wenzhöfer, F., Peeken, I., Sørensen, H. L., Glud, R. N. and Boetius, A.: Composition, buoyancy regulation and fate of ice algal aggregates in the Central Arctic Ocean, *PLoS One*, 9, doi:10.1371/journal.pone.0107452, 2014.
- Friese, E. and Ebel, A.: Temperature dependent thermodynamic model of the system $H^+ - NH_4 - Na^+ - SO_4^{2-} - NO_3^- - Cl - H_2O$, *J. Phys. Chem A.*, 114, 11595–11631, doi:10.1021/jp101041j, 2010.
- Galgani, L., Piontek, J. and Engel, A.: Biopolymers form a gelatinous microlayer at the air-sea interface when Arctic sea ice melts, *Sci. Rep.*, 6, 29465, doi:10.1038/srep29465, 2016.
- Irish, V. E., Elizondo, P., Chen, J., Chou, C., Charette, J., Lizotte, M., Ladino, L. A., Wilson, T. W., Gosselin, M., Murray, B. J., Polishchuk, E., Abbatt, J. P. D., Miller, L. A. and Bertram, A. K.: Ice-nucleating particles in Canadian Arctic sea-surface microlayer and bulk seawater, *Atmos. Chem. Phys.*, 17, 10583–10595, doi:10.5194/acp-17-10583-2017, 2017.
- Knopf, D. A., Alpert, P. A., Wang, B. and Aller, J. Y.: Stimulation of ice nucleation by marine diatoms, *Nat. Geosci.*, 4, 88–90, doi:10.1038/ngeo1037, 2011.
- Koop, T. and Zobrist, B.: Parameterizations for ice nucleation in biological and atmospheric systems., *Phys. Chem. Chem. Phys.*, 11, 10839–10850, doi:10.1039/b914289d, 2009.
- Koop, T., Luo, B., Biermann, U. M., Crutzen, P. J. and Peter, T.: Freezing of $HNO_3 / H_2SO_4 / H_2O$ Solutions at Stratospheric Temperatures: Nucleation Statistics and Experiments, *J. Phys. Chem. A*, 101, 1117–1133, doi:10.1021/jp9626531, 1997.
- Koop, T., Ng, H. P., Molina, L. T. and Molina, M. J.: A New Optical Technique to Study Aerosol Phase Transitions: The Nucleation of Ice from H_2SO_4 Aerosols, *J. Phys. Chem. A*, 102, 8924–8931, doi:10.1021/jp9828078, 1998.
- Kumar, A., Marcolli, C., Luo, B. and Peter, T.: Ice nucleation activity of silicates and aluminosilicates in pure water and aqueous solutions – Part 1: The K-feldspar microcline, *Atmos. Chem. Phys.*, 18, 7057–7079, doi:10.5194/acp-18-7057-2018, 2018.
- Lewis, E. R. and Schwartz, S. E.: Sea salt aerosol production: mechanisms, methods, measurements and models - a critical



- review, American Geophysical Union, Washington, DC., 2004.
- Lohmann, U.: A glaciation indirect aerosol effect caused by soot aerosols, *Geophys. Res. Lett.*, 29, 1052, doi:10.1029/2001gl014357, 2002.
- Lohmann, U. and Feichter, J.: Global indirect aerosol effects: a review, *Atmos. Chem. Phys.*, 5, 715–737, doi:10.5194/acpd-5 4-7561-2004, 2005.
- Marie, D., Simon, N. and Vaultot, D.: Phytoplankton cell counting by flow cytometry, in *Algal Culturing Techniques*, 253–267, Academic Press, London., 2005.
- Rosinski, J., Haagenson, P. L., Nagamoto, C. T. and Parungo, F.: Ice-forming nuclei of maritime origin, *J. Aerosol Sci.*, 17, 23–46, doi:10.1016/0021-8502(86)90004-2, 1986.
- 10 Rosinski, J., Haagenson, P. L., Nagamoto, C. T. and Parungo, F.: Nature of ice-forming nuclei in marine air masses, *J. Aerosol Sci.*, 18, 291–309, doi:10.1016/0021-8502(87)90024-3, 1987.
- Rosinski, J., Haagenson, P. L., Nagamoto, C. T., Quintana, B., Parungo, F. and Hoyt, S. D.: Ice-forming nuclei in air masses over the Gulf of Mexico, *J. Aerosol Sci.*, 19, 539–551, 1988.
- Schnell, R. C.: Ice Nuclei in Seawater, Fog Water and Marine Air off the Coast of Nova Scotia: Summer 1975, *J. Atmos. Sci.*, 34, 1299–1305, 1977.
- 15 Schnell, R. C. and Vali, G.: Freezing nuclei in marine waters, *Tellus*, 27, 321–323, doi:10.3402/tellusa.v27i3.9911, 1975.
- Schnell, R. C. and Vali, G.: Biogenic Ice Nuclei: Part I. Terrestrial and Marine Sources, *J. Atmos. Sci.*, 33, 1554–1564, doi:10.1175/1520-0469(1976)033<1554:BINPIT>2.0.CO;2, 1976.
- Shinki, M., Wendeberg, M., Vagle, S., Cullen, J. T. and Hore, D. K.: Characterization of adsorbed microlayer thickness on an oceanic glass plate sampler, *Limnol. Oceanogr. Methods*, 10, 728–735, doi:10.4319/lom.2012.10.728, 2012.
- 20 Tan, I., Storelvmo, T. and Zelinka, M. D.: Observational constraints on mixed-phase clouds imply higher climate sensitivity, *Science*, 352, 224–227, 2016.
- Tremblay, G., Belzile, C., Gosselin, M., Poulin, M., Roy, S. and Tremblay, J. É.: Late summer phytoplankton distribution along a 3500 km transect in Canadian Arctic waters: Strong numerical dominance by picoeukaryotes, *Aquat. Microb. Ecol.*, 25 54, 55–70, doi:10.3354/ame01257, 2009.
- Vali, G.: Quantitative Evaluation of Experimental Results on the Heterogeneous Freezing Nucleation of Supercooled Liquids, *J. Atmos. Sci.*, 28, 402–409, 1971.
- Wang, X., Sultana, C. M., Trueblood, J., Hill, T. C. J., Malfatti, F., Lee, C., Laskina, O., Moore, K. A., Beall, C. M., McCluskey, C. S., Cornwell, G. C., Zhou, Y., Cox, J. L., Pendergraft, M. A., Santander, M. V., Bertram, T. H., Cappa, C. D., 30 Azam, F., DeMott, P. J., Grassian, V. H. and Prather, K. A.: Microbial Control of Sea Spray Aerosol Composition: A Tale of Two Blooms, *ACS Cent. Sci.*, 1, 124–131, doi:10.1021/acscentsci.5b00148, 2015.
- Wexler, A. S. and Clegg, S. L.: Atmospheric aerosol models for systems including the ions H^+ , NH_4^+ , Na^+ , SO_4^{2-} , NO_3^- , Cl^- , Br^- , and H_2O , *J. Geophys. Res.*, 107, 4207, doi:10.1029/2001JD000451, 2002.
- Whale, T. F., Murray, B. J., O’Sullivan, D., Wilson, T. W., Umo, N. S., Baustian, K. J., Atkinson, J. D., Workneh, D. A. and



- Morris, G. J.: A technique for quantifying heterogeneous ice nucleation in microlitre supercooled water droplets, *Atmos. Meas. Tech.*, 8, 2437–2447, doi:10.5194/amt-8-2437-2015, 2015.
- Wilson, T. W., Ladino, L. A., Alpert, P. A., Breckels, M. N., Brooks, I. M., Browse, J., Burrows, S. M., Carslaw, K. S., Huffman, J. A., Judd, C., Kilhau, W. P., Mason, R. H., McFiggans, G., Miller, L. A., Nájera, J. J., Polishchuk, E., Rae, S., Schiller, C. L., Si, M., Temprado, J. V., Whale, T. F., Wong, J. P. S., Wurl, O., Yakobi-Hancock, J. D., Abbatt, J. P. D., Aller, J. Y., Bertram, A. K., Knopf, D. A. and Murray, B. J.: A marine biogenic source of atmospheric ice-nucleating particles, *Nature*, 525, 234–238, doi:10.1038/nature14986, 2015.
- Yun, Y. and Penner, J. E.: An evaluation of the potential radiative forcing and climatic impact of marine organic aerosols as heterogeneous ice nuclei, *Geophys. Res. Lett.*, 40, 4121–4126, doi:10.1002/grl.50794, 2013.
- 10 Zobrist, B., Marcolli, C., Peter, T. and Koop, T.: Heterogeneous ice nucleation in aqueous solutions: the role of water activity., *J. Phys. Chem. A*, 112, 3965–75, doi:10.1021/jp7112208, 2008.



Station number	Sampling start time (UTC)*	Location
Station 1	20 th July 2016 18:30	60°17.921N 062°10.750W
Station 2	28 th July 2016 15:30	67°23.466N 063°22.067W
Station 3	1 st August 2016 13:30	71°17.200N 070°30.236W
Station 4	6 th August 2016 13:30	76°20.341N 071°11.418W
Station 5	8 th August 2016 11:00	76°43.777N 071°47.267W
Station 6	9 th August 2016 14:30	76°18.789N 075°42.963W
Station 7	11 th August 2016 17:00	77°47.213N 076°29.841W
Station 8	13 th August 2016 10:30	81°20.041N 062°40.774W
Station 9	15 th August 2016 14:00	78°18.659N 074°33.757W
Station 10	21 st August 2016 10:00	68°19.199N 100°49.010W
Station 11	23 rd August 2016 10:30	68°58.699N 105°30.022W

Table 1. Sampling times and geographic coordinates for the eleven stations investigated.



	Microlayer T ₁₀ -value			Bulk T ₁₀ -value		
	r	p	n	r	p	n
Heterotrophic bacterial abundance	-0.42	0.100	11	-0.77	0.003	11
Total phytoplankton abundance (0.2 - 20 μm)	-0.06	0.436	11	0.19	0.287	11
Salinity	-0.74	0.005	11	-0.83	0.001	11
Temperature	n/a	n/a	n/a	0.20	0.285	10

Table 2. Correlations between biological and physical properties of microlayer and bulk seawater and T₁₀-values for 2016. Values in bold indicate results that are statistically significant. The symbol n/a represents correlations for which there were no data.

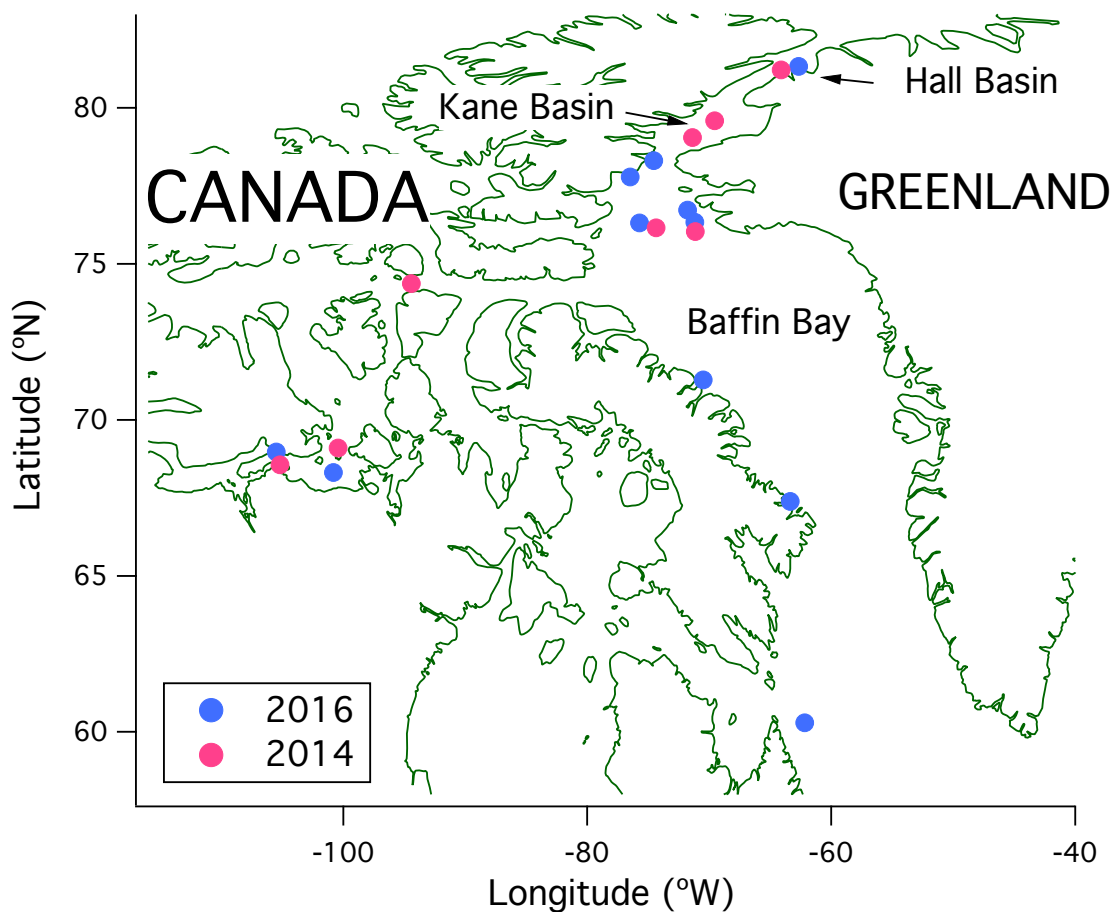


Figure 1. Map showing locations of microlayer and bulk seawater sampling in 2014 (pink) and 2016 (light blue).

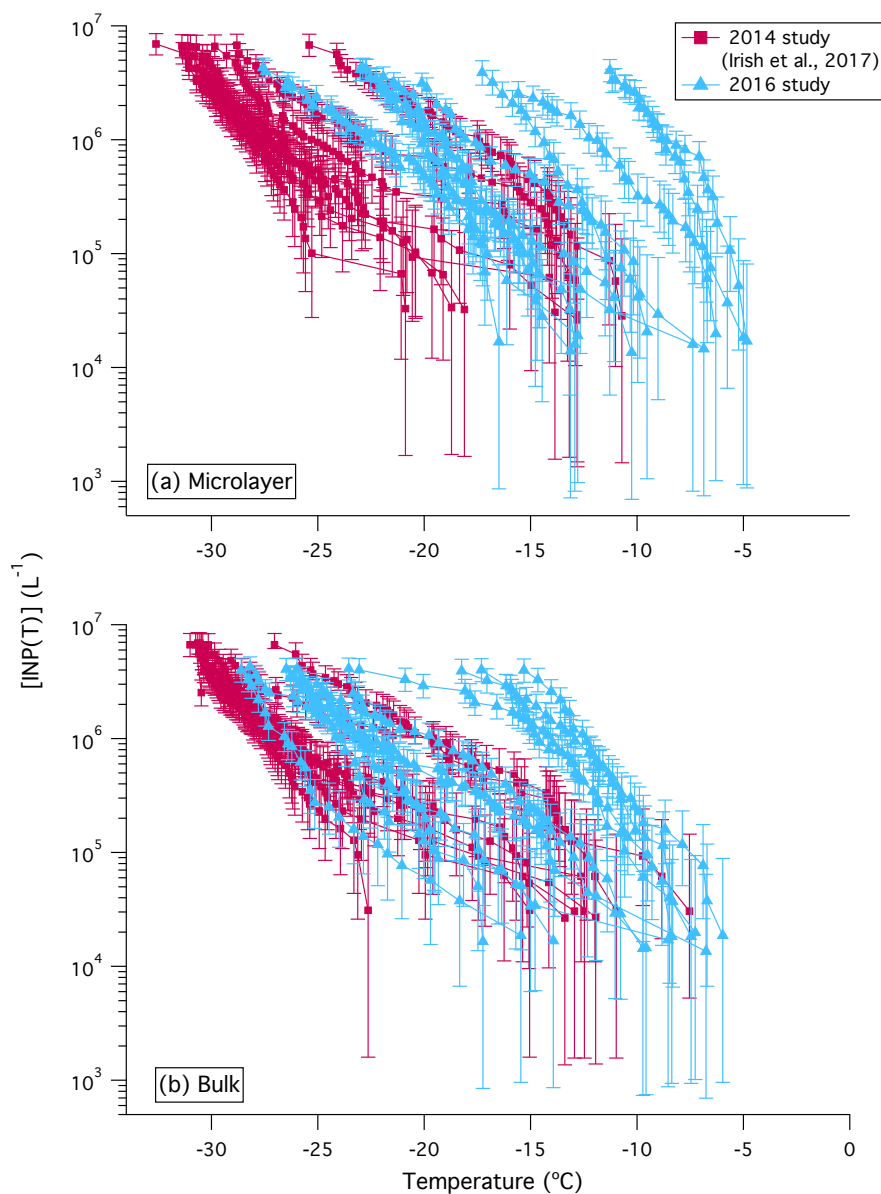


Figure 2. Comparison of the concentrations of INPs, $[\text{INP}(T)]$, in (a) the microlayer and (b) bulk seawater samples from the 2014 study (pink squares) and the 2016 study (blue triangles). All data are corrected for freezing point depression. Error bars represent the statistical uncertainty due to the limited number of nucleation events observed in the freezing experiments (Koop et al., 1997).

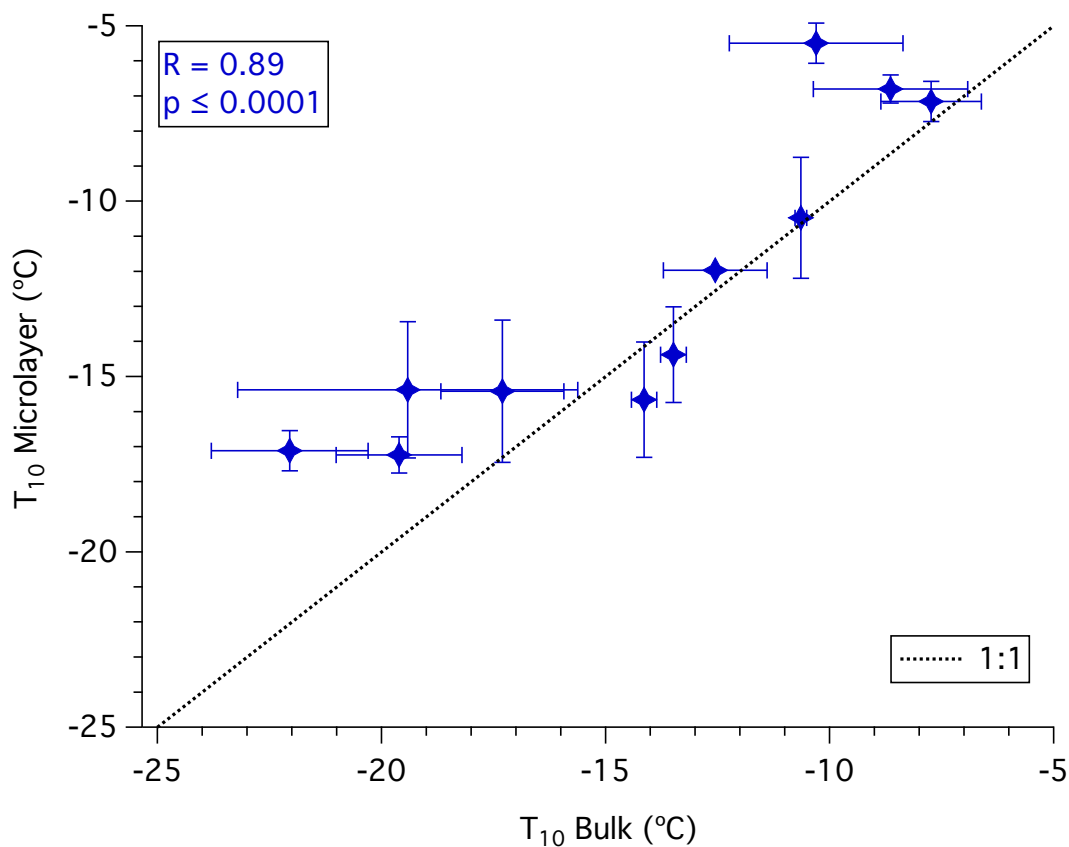


Figure 3. Relationship between T_{10} -values for microlayer and bulk seawater samples with a 1:1 line for reference. Data points are the average T_{10} -values from three repeat experiments. Error bars are the 95% confidence interval for three repeat experiments.

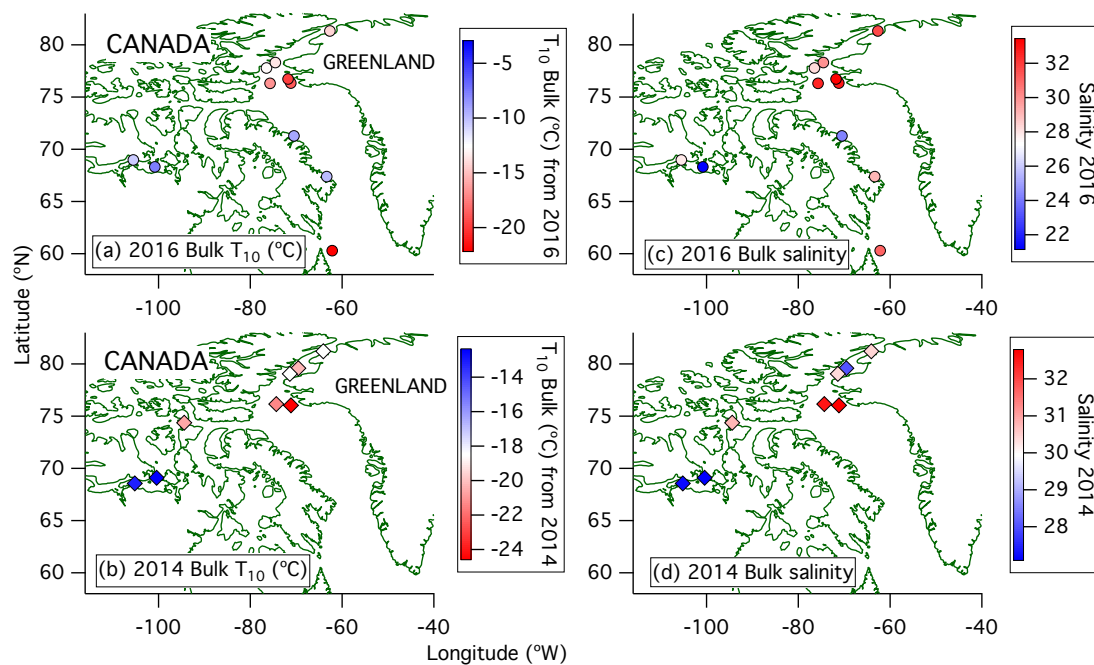


Figure 4. Spatial patterns of (a, b) T_{10} -values and (c, d) salinities in (a, c) 2016 and (b, d) 2014 for bulk seawater.

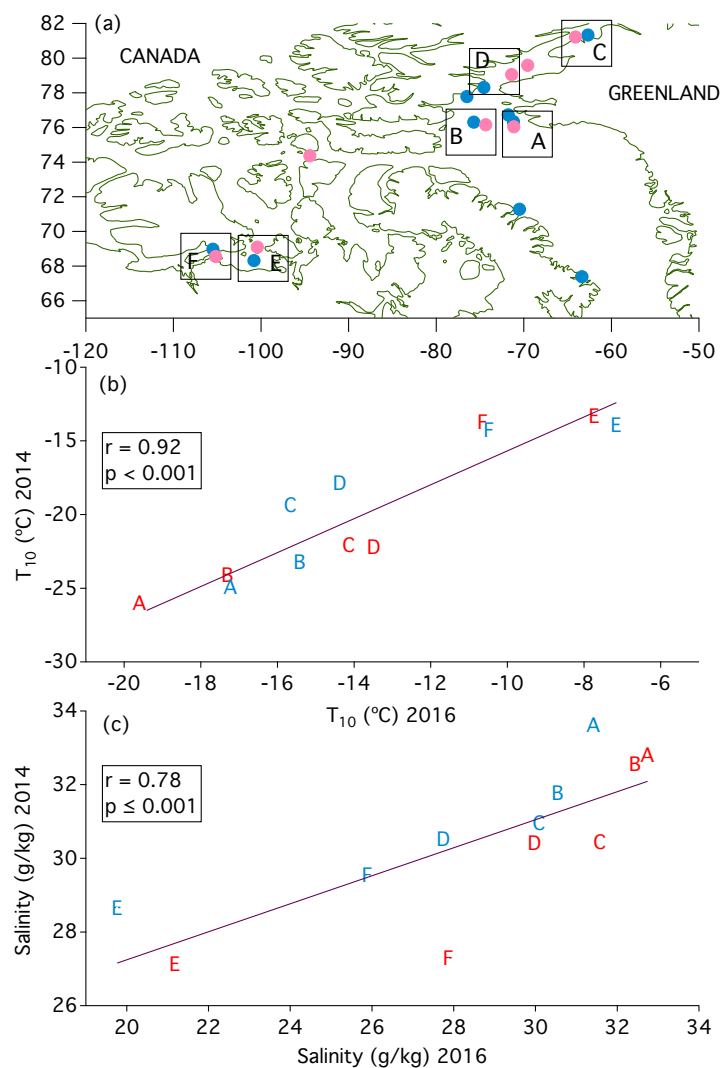


Figure 5. (a) Map showing regions of similar sampling locations in 2014 (pink) and in 2016 (blue). Sampling sites in 2014 that were near sampling sites in 2016 were paired together (indicated with boxes in the figure) and assigned letters A-F. Although there are two stations in box A for 2016, we only used data for the station that was closest to the one in 2014. Relationships between (b) T_{10} -values, and (c) salinities for microlayer and bulk seawater samples in 2014 and 2016 for similar sampling locations. The letters plotted in (b) and (c) indicate the locations in (a). Red letters represent bulk seawater data and blue letters represent microlayer data.

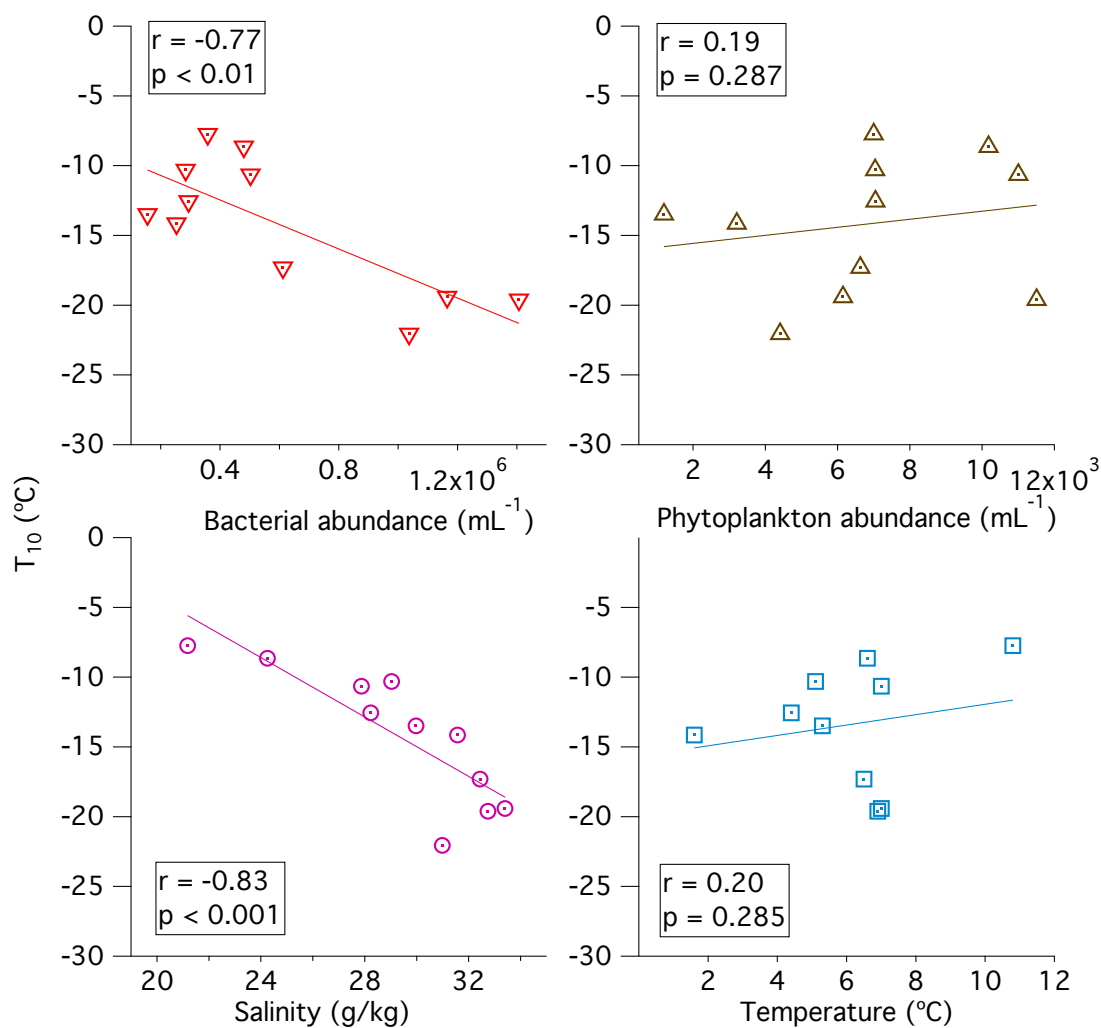


Figure 6. Relationships between biological and physical properties of bulk seawater and T_{10} -values for the 2016 study.

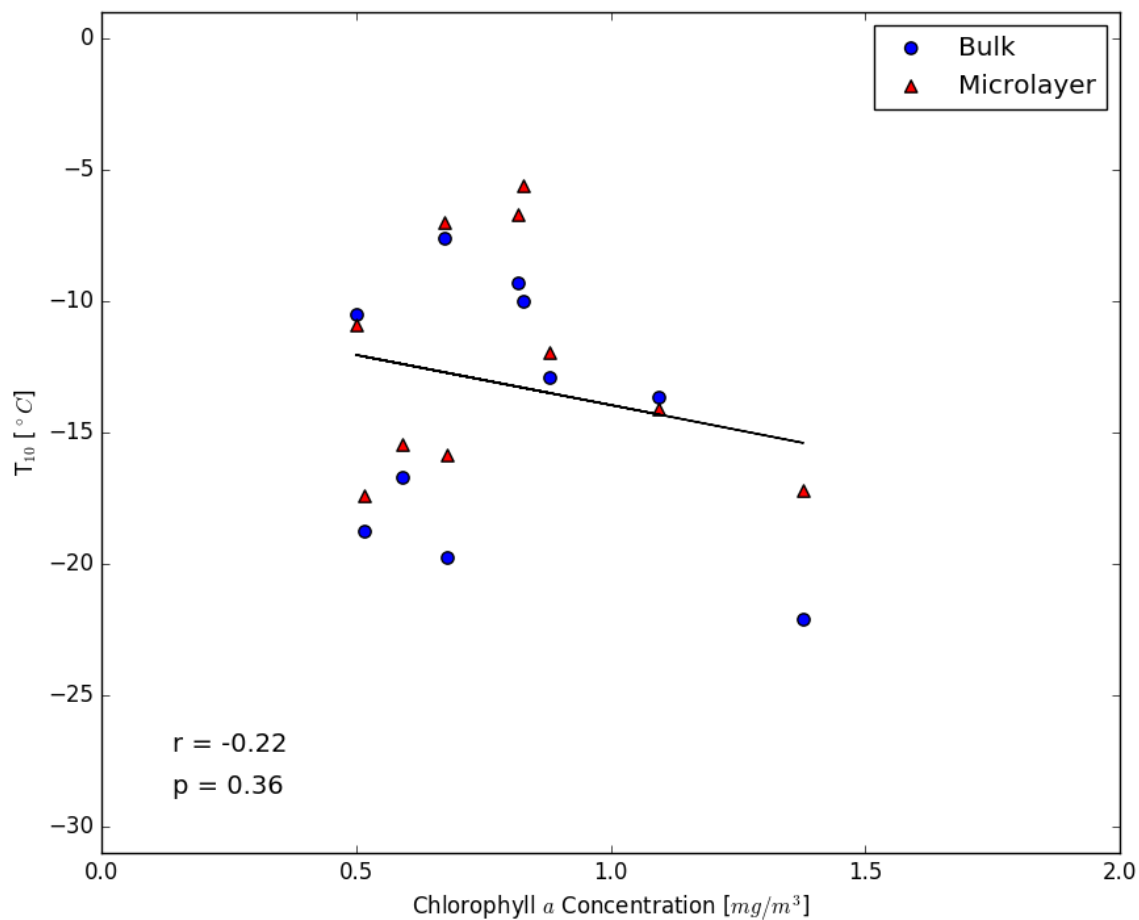


Figure 7. Relationship between chlorophyll *a* concentrations derived from satellite imagery from the GlobColour project and the T_{10} -values of microlayer and bulk seawater for 2016.